

Arcalís: Accelerating Remote Procedure Calls Using a Lightweight Near-Cache Solution

Johnson Umeike

University of Maryland,
College Park, USA
jumeike@umd.edu

Pongstorn Maidee

AMD Research & Advanced Development
San Jose, CA, USA
pongstorn.maidee@amd.com

Bahar Asgari

University of Maryland,
College Park, USA
bahar@umd.edu

Abstract—Modern microservices increasingly depend on high-performance remote procedure calls (RPCs) to coordinate fine-grained, distributed computation. As network bandwidths continue to scale, the CPU overhead associated with RPC processing, particularly serialization, deserialization, and protocol handling, has become a critical bottleneck. This challenge is exacerbated by fast user-space networking stacks such as DPDK, which expose RPC processing as the dominant performance limiter. While prior work has explored software optimizations and FPGA-based offload engines, these approaches remain physically distant from the CPU’s memory hierarchy, incurring unnecessary data movement and cache pollution. We present Arcalís, a near-cache RPC accelerator that positions a lightweight hardware engine adjacent to the last-level cache (LLC). Arcalís offloads RPC processing to dedicated microengines on receive and transmit paths that operate with cache-line latency while preserving programmability. By decoupling RPC processing logic, enabling microservice-specific execution, and positioning itself near the LLC to immediately consume data injected by network cards, Arcalís achieves 1.79–4.16× end-to-end speedup compared to the CPU baseline, while significantly reducing microarchitectural overhead by up to 88%, and achieves up to a 1.62× higher throughput than prior solutions. These results highlight the potential of near-cache RPC acceleration as a practical solution for high-performance microservice deployment.

I. INTRODUCTION

Modern datacenter applications are increasingly built using *microservices*, which are independently deployable components that communicate through remote procedure calls (RPCs). Compared to monolithic architectures, microservices offer better modularity, scalability, and deployment flexibility [28], [70]. Figure 1 illustrates how microservices interact through language-agnostic RPC stubs, enabling a Python-based client to invoke functionality implemented in a C++ service. This cross-language abstraction simplifies distributed development but also introduces substantial software and communication overhead into every request. However, this decomposition comes at a cost: the performance overhead of frequent inter-service communication via RPCs, now referred to as the “*RPC tax*” [40], [63], [65]. The RPC tax manifests in multiple forms across the system stack. At the application level, microservices spend 18–94% of their execution time in RPC processing rather than in business logic [33], [63]. At the microarchitectural level, RPC workloads exhibit poor instruction locality, high branch misprediction rates, and memory-bound execution



Fig. 1: *RPC enables cross-language, platform-independent communication between heterogenous microservices.*

patterns [52], [70]. Our microarchitectural analysis reveals that even with optimized userspace networking stacks like DPDK [16], up to 67.6% of pipeline slots are lost to frontend bottlenecks and memory hierarchy stalls, with only 47.9% achieving productive instruction retirement in the best case (Section III-A).

The problem is exacerbated by the growing deployment of high-performance networking technologies. Userspace networking frameworks (DPDK [16], Snap [50], IX [7], ZygOS [64]) and hardware-accelerated transports (RDMA [57], InfiniBand [58], RoCE [59]) eliminate kernel bottlenecks but expose RPC processing as the dominant performance limiter [45], [80]. The serialization/deserialization layer alone consumes up to 94% of RPC processing cycles [63], arising from both nested and single RPC layers. This creates a fundamental mismatch between network capability and application performance. To address these limitations, researchers have proposed various RPC acceleration approaches (Table I), each with distinct trade-offs:

NICs-attached accelerators such as Cerebros [63], Optimus Prime [62], and NeBuLa [71] offload RPC processing to smart NICs, significantly reducing CPU overhead. However, their fixed-function architectures limit adaptability to evolving protocols, data formats, and dynamic microservice environments that frequently update service interfaces.

On-chip accelerators such as ProtoAcc [41] integrate custom logic directly within the CPU, offering ultra-low latency through tight coupling with the processor pipeline.

While effective, they require invasive changes to commodity CPUs, creating deployment barriers and limiting scalability across heterogeneous datacenter infrastructures.

FPGA-based solutions provide reconfigurability and high throughput. Dagger [45] leverages specialized NUMA interconnects (UPI) to achieve 400 ns access latency;

however, it requires tight memory hierarchy integration, which complicates deployment and uses special interconnect. RpcNIC [80] proposes a more general PCIe-connected architecture. To mitigate the high-latency cost of PCIe

TABLE I: Comparison of RPC acceleration proposals.

RPC Acceleration Proposal	Design Features	Flexible / Programmable	Full RPC Offload	Cache-Line Access Latency
eRPC [38]	S	✓	N/A	N/A
Optimus Prime [62]	N	✗	✗	✗
Cerebros [63]	N	✗	✓	✗
ProtoAcc [41]	OC	✗	✗	✓
Dagger [45]	F	✓	✓	✗
RpcNIC [80]	N, F	✓	✓	✗
NeBuLa [71]	N	✗	✓	✗
<i>Arcalís</i>	OC, F, NL	✓	✓	✓

Symbols: S = Software-based, N = NIC-attached, F = FPGA-based, OC = On-chip, NL = Near-LLC.

traversal (≈ 900 ns) reported in prior work [54], it splits RPC processing between the host CPU and the accelerator. Its design also depends on CPU-integrated on-chip memcpy engines. Consequently, RpcNIC does not completely offload RPC processing from the CPU and is only applicable to systems with CPUs that are equipped with memcpy engines, a feature that is not widely available.

Software-only approaches such as FARM [19], eRPC [38] and FaSST [39] optimize RPC performance through kernel-bypass networking and efficient software stacks. While offering low deployment barriers, these solutions still consume substantial CPU resources and cannot match the performance isolation of hardware-assisted designs under high loads.

The fundamental challenge is that existing solutions either sacrifice flexibility for performance (i.e. fixed-function accelerators), incur data movement overhead, or sacrifice performance for deployability (software approaches).

Recent I/O techniques allow Network Interface Cards (NICs) to place data directly into the CPU cache hierarchy. To fully eliminate unnecessary data movement, RPC handling should occur as close to the cache as possible. The main obstacle to achieving this efficiency is that a generic solution is too large to be integrated at that proximity. Running a service on servers that recently executed it improves performance by avoiding cold starts [37]. In particular, stateful microservices—databases and key-value stores like Memcached—are often deployed on dedicated servers to avoid migrating large amounts of state [49]. In those cases, it is sensible to configure the accelerator specifically for the services currently running on the CPUs.

Taking advantage of these insights, we present *Arcalís*, which makes three main contributions: (1) The first RPC accelerator that eliminates data movement overhead. *Arcalís* is a lightweight hardware engine located adjacent to the last-level cache, featuring configurable RxEngine/TxEngine processing pipelines that achieve cache-line access latency while maintaining programmability through systematic hardware-software co-design. (2) A comprehensive analysis of RPC bottlenecks revealing fundamental microarchitectural inefficiencies in modern processor pipelines. (3) Microarchitectural insights demonstrate that near-cache acceleration fundamentally improves processor

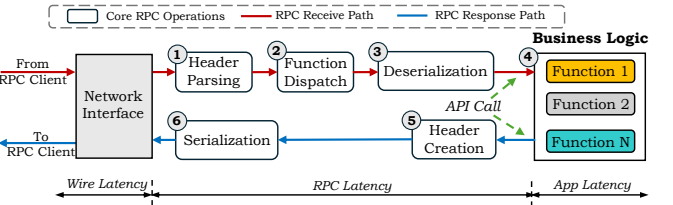


Fig. 2: RPC processing pipeline in modern microservices deployments. Stages 1-3, 5-6 are implemented within standard RPC frameworks [4], [30].

efficiency, reducing instruction count by 65-86%, load-to-use latency by 63-88%, and cache access overhead by 61-87%. Evaluation shows that *Arcalís* achieves 1.79-4.16 \times end-to-end performance improvements.

II. BACKGROUND

This section outlines the architectural shifts and system level trends that shape the modern RPC execution path. Our goal is to expose structural inefficiencies that arise from treating communication and computation as separate layers, inefficiencies that become unsustainable as datacenter networks outpace memory systems and software stacks. These trends highlight the need to revisit long standing assumptions about how performance critical communication workloads interact with hardware.

RPC Processing in Modern Microservices. Early RPC frameworks such as Sun RPC [78] and CORBA [77] prioritized simplicity and Local Area Network (LAN) compatibility, using fixed-format messages and basic marshalling schemes tailored for homogeneous systems. In contrast, modern cloud applications rely on microservices, where high-frequency RPCs orchestrate fine-grained interactions among loosely coupled services [28], [75], [81], [83]. These RPCs operate with tight latency budgets [82] and are mediated by frameworks such as Thrift [4], gRPC [30], and Cap'n Proto [11], which support schema evolution, type safety, and multi-language bindings. However, these features introduce layered processing overheads that translate into real resource costs at scale. As illustrated in Figure 2, a

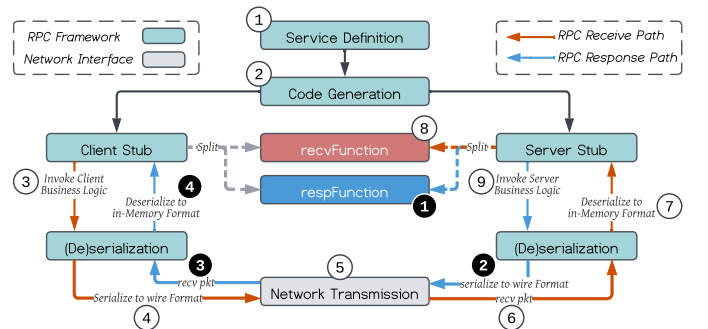


Fig. 3: RPC communication workflow. After service definition and code generation (steps 1-2), the client invokes a remote function, which must go through serialization, network transmission, and deserialization (steps 3-6). The server processes the request and returns a response following the reverse path (steps 7-9), with client and server stubs abstracting the underlying communication.

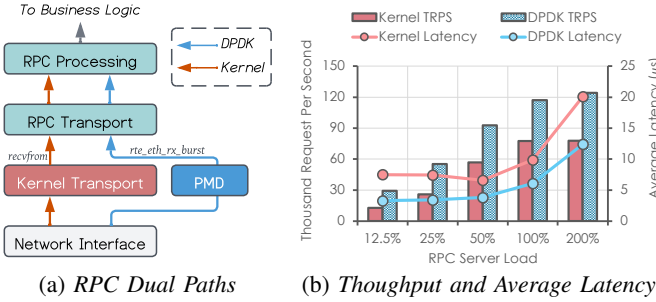


Fig. 4: Effectiveness of Kernel-Bypass Networking for RPC Execution: (a) Kernel and DPDK Receive RPC Processing Paths. DPDK directly access the Network Interface hardware using its Poll Mode Driver (PMD) (b) Throughput (Thousand Requests Per Second) and Average Latency for Memcached RPC (0.8 SET ratio) using DPDK and Kernel Networking.)

typical RPC call at the server traverses six structured software stages: header parsing (1) extracts metadata such as function name and request ID; function dispatch (2) invokes the appropriate handler from a function table; deserialization (3) reconstructs in-memory objects from the wire format; business logic (4) performs the core computation (e.g. SET or GET in the case of memcached); header creation (5) attaches protocol metadata for reply transmission; and serialization (6) encodes the response back to wire format. These steps involve predictable but compute- and memory-intensive tasks, including schema-driven field parsing and dynamic function resolution [42], [62]. Profiling studies show that the core RPC operations account for a significant fraction of per-request latency and CPU cycles in production systems [27], [70], [72], making structured RPC handling a major source of inefficiency at scale.

Figure 3 illustrates how modern RPC frameworks generate the client and server stubs that handle each request. Although the compiler emits a single stub on each side, the code naturally separates into two logical components, a *recvFunction* that interfaces with the framework’s receive path for header parsing and deserialization, and a *respFunction* that allows for corresponding header construction and serialization on the response path. Later, we will show how *Arcalis* exploits this structure to offload RPC handling to a near-cache engine.

Datacenter I/O Optimizations. Modern datacenters have adopted high-speed interconnects and kernel-bypass techniques to reduce communication overhead. Technologies such as DPDK [16], Snap [50], and mTCP [36] enable applications to send and receive packets directly from userspace, bypassing the kernel networking stack. These frameworks reduce context switches, memory copies, and interrupt overhead, achieving packet latencies on the order of microseconds and throughput scaling into tens of millions of requests per second [7], [26], [60], [64].

Figure 4a differentiates the kernel and DPDK RPC receive paths. In the kernel stack, packets traverse the NIC driver, kernel transport, and socket layer before reaching the RPC runtime. DPDK bypasses these layers entirely, allowing

a poll-mode driver (PMD) to pull packets directly into userspace and hand them to the RPC framework, completely avoiding interrupts, data copying, and dynamic skb allocation overheads [10]. As shown in Figure 4b, which shows that DPDK achieves higher request throughput and lower average latency across a wide range of server loads. While both paths eventually saturate the core, the kernel stack incurs additional queuing and scheduling overheads, causing latency to rise sharply under load. RDMA-based solutions such as InfiniBand [58] and RoCE [59] also bypass the kernel network stack, providing direct memory access between machines without CPU intervention. They both leverage specialized NIC hardware and transport engines to perform reliable communication with sub-us latency.

To meet the demands of high-speed networks, recent innovations have focused on reducing CPU-side memory access costs during packet processing. Techniques such as AMD’s smart data cache injection (SDCI)¹ [2], Intel’s data direct I/O (DDIO) [34], and Arm’s cache stashing [6] allow network devices to inject incoming packets directly into the processor’s cache. These direct cache access (DCA) mechanisms bypass DRAM, reducing latency and memory bandwidth usage. Inbound DMA writes use a write-allocate/write-update (WAU) policy to place I/O data directly into the LLC [24]. If the cache line already exists, it is updated in place and marked as dirty. Otherwise, it is allocated in a reserved LLC portion. The line remains in cache and is written back to DRAM only upon eviction. By avoiding costly DMA round-trips to system memory, DCA enhances the efficiency of CPU-bound microservices and enables better overlap between network and computation tasks [48].

Accelerator Integration Models. The trend toward domain-specific acceleration has driven the exploration of different accelerator placement strategies within the system hierarchy, each offering distinct trade-offs between performance, cost, and integration complexity. These range from peripheral accelerators connected via PCIe [22], [25], to near-memory processing elements positioned at memory controllers [1], [29], to on-chip accelerators integrated within the processor package [12], [23]. Each placement offers different latency, bandwidth, and coherency characteristics that impact workload suitability. For RPC processing specifically, while existing approaches span this placement spectrum [45], [63], [71], [80], they face fundamental limitations: peripheral solutions suffer from PCIe latency penalties, while existing on-chip designs lack tight integration with processor cache hierarchies.

III. OPPORTUNITIES FOR NEAR-CACHE ACCELERATION

A. Characterizing RPC Processing Bottlenecks

CPUs are inefficient at processing RPCs due to microarchitectural mismatches between their general-purpose design and the characteristics of RPC workloads. Prior profiling studies of WSC systems reveal that RPC execution

¹AMD, the AMD Arrow logo and combinations thereof are trademarks of Advanced Micro Devices, Inc.

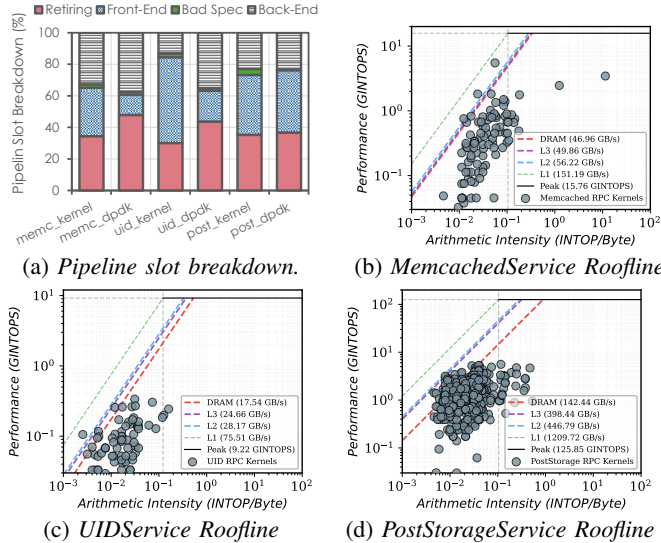


Fig. 5: Performance Characterization of RPC Microservices: (a) Pipeline slot utilization showing front-end and back-end stalls, (b)-(d) Roofline analysis demonstrating memory bandwidth bottlenecks in kernel execution

suffers from high instruction-fetch overheads, front-end stalls, cache misses, and backend latency [13], [27], [63], [65]. Over 30% of pipeline slots are often stalled at the front-end, and backend cycles are frequently consumed by L1 cache misses and TLB pressure [40]. These issues are amplified in microservice-style designs with frequent inter-service RPCs. To understand the microarchitectural inefficiencies of RPC execution and the impact of user-level networking, we profile *Memcached* [51] and representative microservices from DeathStarBench [28], including *PostStorageService*, and *UniqueIdService*, on a server (Table II) hosted on a research testbed [20].

TABLE II: Server hardware configuration used for evaluation.

Component	Specification
CPU	Intel Xeon Silver 4314 (2.4 GHz, 16 cores / 32 threads)
Memory	128 GB DDR4-3200 ECC (8 channels, 170.6 GB/s peak)
NIC	Dual-port Mellanox ConnectX-6 DX (100 GbE per port)

Fig. 5a shows the pipeline breakdown across six RPC-centric services in our study. In the best case, only 47.9% of slots retire instructions; the rest are lost to front-end bottlenecks, branch resteers, and backend stalls. Notably, up to 12% of cycles are spent waiting on the memory hierarchy, including DRAM latency, store buffers, and L1-bound stalls. These results persist even when kernel overhead is removed via userspace networking. While prior works examine kernel-mode RPC stacks and/or coarse-grained system profiling, our study is the first to combine top-down hardware pipeline analysis with user-level networking stacks such as DPDK.

Figures 5b-5d show that RPC kernels operate at very low arithmetic intensities, between 10^{-3} and 10^1 GINTOP/Byte, placing them squarely in the memory-bound region of the roofline. Their achieved performance remains below the compute roof and never approaches the L1 or L2 bandwidth ceilings, indicating that computation is not the

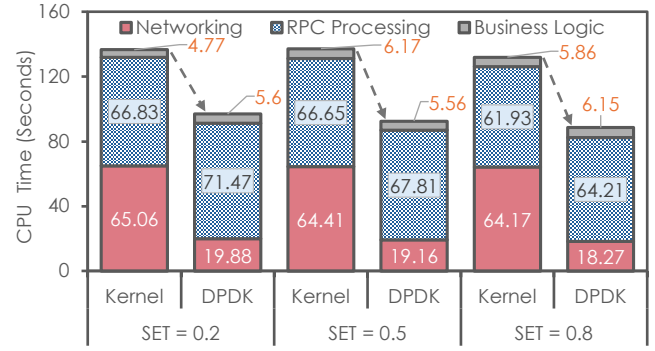


Fig. 6: CPU time breakdown for Memcached processing 10 million RPC requests across SET ratios.

limiting factor. Instead, these kernels are dominated by fine-grained metadata accesses and pointer-heavy operations that generate poor spatial locality and frequent cache misses. This behavior aligns with the pipeline-slot breakdown and highlights that RPC execution on general-purpose cores is fundamentally constrained by memory latency rather than compute throughput.

An additional source of inefficiency originates from the way RPC logic is interleaved with the business logic on the CPU. The mixing performed on each request introduces transient instruction and data accesses that disrupt locality, evict useful cache lines, and amplify the memory-bound behavior seen in the roofline analysis. This interaction increases I-cache and ITLB pressure and contributes to the memory stalls observed in the pipeline breakdown. Prior accelerator efforts that focus only on software overheads or (De)serialization [45], [62], [63] do not eliminate these effects because the CPU still executes the RPC path. Together, these observations point to the need for moving RPC handling into the near-cache region, where it can avoid these stalls and free the core for business logic.

B. When Zero-Copy Is Not Zero-Cost

High-performance networking frameworks such as DPDK eliminate the kernel from the critical path and leverage zero-copy DMA techniques to boost throughput. Prior work has thoroughly characterized kernel-mode RPC overheads, identifying memory copies and TCP/IP stack processing as dominant bottlenecks on the receiver side [10], [69]. DPDK mitigates these issues using hugepages and direct NIC-to-user memory access, dramatically improving packet delivery. However, as shown in Fig. 6, removing kernel overheads now exposes the RPC layer as the dominant bottleneck.

We profile CPU time across the network stack, Thrift RPC layer, and business logic while serving 10 million requests in *Memcached* microservice under different set ratios (20%, 50%, & 80%). When using kernel networking, a large portion of CPU time (~50%) is spent in the slow kernel network stack. With DPDK [16], the kernel overhead is largely eliminated, reducing total network time by 3.38 \times on average. However, the time spent in RPC processing slightly increases and becomes the dominant component of the total execution time, while the business logic component

remains effectively unchanged. This shift highlights that while userspace networking improves packet handling efficiency, it exposes the serialization and deserialization overheads in the RPC layer, revealing the inefficiency of executing these tasks entirely on general-purpose CPU cores.

Moreover, at higher packet ingress rates, the CPU becomes more exposed to frequent cache line loads and memory pressure. This mirrors the broader “datacenter tax” effect, where even efficient packet delivery translates into heavier application processing burdens [7], [60]. Our results empirically reinforce this by showing that, despite lower stack overhead, user-level networking inflates the total CPU burden.

C. Why DMA Isn’t enough

DMA-attached accelerators, such as SmartNICs and PCIe-based FPGAs, are a common method for offloading compute and packet processing tasks in datacenters. These devices access memory via DMA, requiring data to be explicitly copied from host buffers, processed on the accelerator, and copied back. While effective for batch or coarse-grained workloads, this model introduces higher overheads for fine-grained microservices. Because these accelerators are decoupled from the CPU cache hierarchy, each invocation incurs buffer orchestration, memory synchronization, and data transfer latency [67]. These costs are particularly pronounced for short-lived RPCs, which involve small messages and frequent core interactions.

To address these limitations, many recent efforts across domains such as graph analytics, stencil computation, deep learning inference, and stream processing have proposed near-cache or cache-coherent accelerators [18], [35], [56], [76] to integrate compute units closer to the core, maintain coherence with the CPU cache hierarchy, and eliminate data movement setup overheads. *Arcalís* adopts a similar philosophy, embedding a cache-coherent compute engine directly within the SoC. Such integration leverages direct cache injection to enable scalable, low-latency RPC acceleration.

IV. ARCALIS: A NEAR-CACHE RPC ACCELERATOR

This section presents the design and architecture of *Arcalís*, our proposed near-cache accelerator that addresses the fundamental RPC processing bottlenecks identified in microservice-based datacenter systems. Building on our analysis from Section III-A, *Arcalís* eliminates the RPC tax through a full-stack hardware offload while preserving compatibility with existing RPC software frameworks and network transport stacks.

Arcalís is driven by four key architectural goals: (G1) completely eliminate CPU involvement in the RPC processing; (G2) enable efficient hardware resource utilization; (G3) facilitate aggressive, application-aware optimizations while avoiding general-purpose complexity; and (G4) ensure portability and seamless integration with existing hardware mechanisms, RPC runtimes, and networking stacks. The remainder of this section details *Arcalís*’s architecture (§4.1), its end-to-end RPC processing pipeline (§4.2), and the

implementation of *Arcalís*, including its hardware modeling in gem5 [8], and software interfaces exposed by microservices to interact with the accelerator (§4.3).

A. Architectural Overview

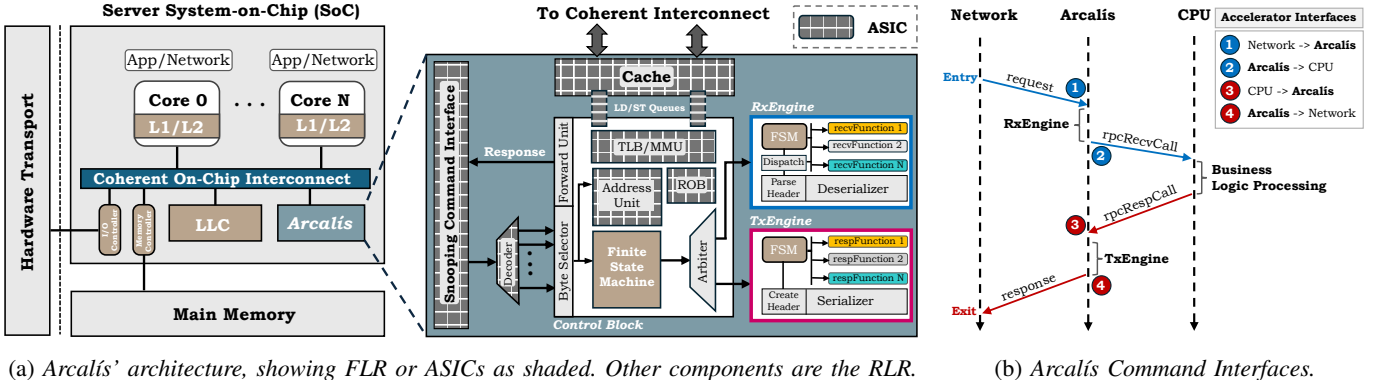
Arcalís represents a paradigm shift in RPC acceleration through its near-cache hardware accelerator, achieving complete RPC layer offload while maintaining tight integration with the server’s memory hierarchy. Figure 7a illustrates the comprehensive architecture of *Arcalís*, which positions itself as a coherent on-chip interconnect component that interfaces directly with both the network infrastructure and CPU cores. Its internal microarchitecture comprises two specialized micro-engines and a shared control block that includes address translation, dispatch, and memory coordination logic.

We adopt a hybrid architecture comprising a *fixed logic region (FLR)* for general-purpose components such as the cache, TLB/MMU, load/store queues, address unit, reorder buffer, and command interface, and a *reconfigurable logic region (RLR)*, containing the offloaded RPC processing logic. We select this partitioning to balance efficiency and flexibility. FPGAs incur area and performance overheads, so reconfigurability is restricted to the components that benefit most from it. The separation also enhances system stability and security, as the *RLR* operates in the virtual address space while the *FLR* handles physical address management.

The accelerator integrates seamlessly into the server’s System-on-Chip (SoC) design, leveraging the coherent interconnect to maintain cache coherency with the CPU cores’ cache hierarchy. This positioning enables *Arcalís* to operate as both a network endpoint and a memory-coherent processing unit, facilitating zero-copy data movement between network packets and application buffers. Next, we discuss the four cardinal design principles around which *Arcalís* is built.

Together, they enable efficient, fully offloaded, and application-specialized RPC execution while ensuring seamless integration with modern SoC memory and network systems.

Complete Hardware Offload: *Arcalís* achieves complete hardware offload by implementing all five critical RPC layer modules (1 - 3, 5 - 6) depicted in Figure 2, entirely in hardware, eliminating the need for CPU involvement in the RPC processing pipeline. Unlike software RPC stacks, which incur multiple system calls, kernel networking, and userspace handler overheads [40], [65], *Arcalís* eliminates the CPU from the critical path of RPCs by implementing the full control and data flow in hardware. This approach addresses the fundamental limitation identified in prior works [62], [63], where partial acceleration creates bottlenecks due to CPU-accelerator coordination overhead. The accelerator maintains four distinct command interfaces as shown in Figure 7b: two interfaces to the network (interfaces 1 and 4) for request ingress and response egress, and two interfaces to the microservice application (interfaces 2 and 3) for CPU communication. Each interface is equipped with dedicated communication buffers that act as in-cache queues, enabling



(a) Arcalis' architecture, showing FLR or ASICs as shaded. Other components are the RLR.

(b) Arcalis Command Interfaces.

Fig. 7: Architecture of the Arcalis near-cache accelerator and its command interfaces. The Fixed Logic Region (FLR) houses the general-purpose ASICs, while the Reconfigurable Logic Region (RLR) implements the micro-engines.

asynchronous, unblocking data exchange between Arcalis and external components. This buffer-based communication model ensures that network packets can be received and processed independently of CPU availability, while responses can be queued for transmission without stalling the processing pipeline.

Specifically, Arcalis leverages *uncacheable* (UC) or *non-temporal* store operations to deliver task descriptors (e.g., buffer address, payload length, and operation code) to memory-mapped command buffers within the accelerator. A corresponding UC load retrieves completion status or result metadata, enabling low-latency synchronization between the network or application and the accelerator. In our design of Arcalis, we reserve the lowest 4 bits of the physical address, within a designated space, to encode the task opcode (Fig. 8), allowing for efficient decoding of the accelerator commands without requiring additional register state or memory transactions. Details regarding the End-to-End execution pipeline are deferred to §IV-C.

Pipeline Decoupling: One of Arcalis's key design principles is the decoupling of the ingress (receive) and egress (response) pipelines, driven by three observations: first, RPC request and response sizes often differ substantially (e.g., large RPC requests and small RPC responses) [65]; second, responses are often generated asynchronously by the CPU following application execution; and third, overlapping ingress and egress processing within the accelerator enables higher utilization and hides idle cycles by allowing multiple RPCs to be in-flight concurrently, in line with (G2). Accordingly, Arcalis divides processing into two independently schedulable datapaths: the RxEngine and the TxEngine, each optimized for its respective phase of RPC handling.

RxEngine, activated via interface (1), handles ingress processing, including header parsing, function ID dispatch, and payload deserialization. Incoming requests from the NIC are deserialized to determine field boundaries and types. This data is then passed to the appropriate microservice-specific recvFunctionN block. On the other hand, TxEngine is responsible for the response path. When the application (microservice business logic) produces a result, TxEngine

is activated via interface (3).

Microservice-Specific Execution Path: Rather than delegating microservice logic to software handlers on the host CPU, we embed specialized recvFunctionN and respFunctionN modules within the accelerator itself (Figure 7a, right). These function blocks are analogous to software RPC handlers but are implemented as lightweight compute datapaths, parameterized per service. Upon receiving an RPC, the RxEngine invokes a recvFunctionN block, which deserializes datafields and performs service-specific processing.

Similarly, the respFunctionN block in TxEngine is invoked directly by the control logic following application-side completion. It encodes the application result, performs structure flattening, and invokes the serializer to compose the wire-format message. By embedding the microservice logic directly into the hardware path, Arcalis eliminates the instruction fetch overhead of software-based RPC handlers [27], [28], [70], [72], [83], while providing the flexibility of software solutions [38], through reconfiguration.

Near-Cache Processing: Arcalis is connected as a coherent agent on the SoC's on-chip interconnect, enabling direct and low-latency access to memory and cache hierarchies. It is physically located near the LLC slices and participates in the memory coherence protocol using LD/ST queues that issue memory operations. These queues are backed by a memory management unit (MMU) and translation lookaside buffer (TLB), which is kept consistent with the host TLB and allows Arcalis to translate virtual addresses into physical addresses, enforce access permissions, and support memory access across distinct user-level address spaces, enabling secure and efficient execution. The reorder buffer (ROB) and Address Unit coordinate multiple outstanding memory transactions, ensuring correct sequencing of dependent operations.

This tight coupling with the LLC enables Arcalis to operate at L1/L2 cache latencies in the best case. Compared to PCIe-attached accelerators [80], Arcalis avoids the long PCIe latency overhead. It acts as a first-class peer to CPU cores and can access data regions with equivalent privileges. This design is especially beneficial for latency-critical microservices,

TABLE III: Commands for data exchange with microservices.

Command Type	Description
CMD_SEND_NET_BUF	Send network packet buffer address
CMD_SEND_NET_LEN	Send packet length metadata
CMD_APP_READY_FLAG	Signal application's readiness for new data
CMD_SEND_APP_RESP	Send application response data
CMD_SEND_APP_BUF	Send application output buffer
CMD_DPDK_NET_FLAG	Signal network's readiness for new data



Fig. 8: 64-bit accelerator command format in *Arcalís*.

where traditional NIC and kernel stacks introduce tens of microseconds of overhead per call [45], [71].

B. Operation and Design of *Arcalís*

We now describe the design of our accelerator and how it integrates into other parts of the system. At a high-level, *Arcalís* comprises the **FLR** and **RLR**, which supports its general-purpose operation and microservice-specific needs, respectively. The accelerator integrates into the memory hierarchy and operates alongside the CPU using a state-driven architecture that monitors specific memory regions and a configuration channel.

a) **Fixed Logic Region**: Forms the ASIC substrate of *Arcalís*, hosting common components across every microservice such as the cache, TLB/MMU, load/store queues, address unit, RoB, and command interface. *Arcalís* operates on two types of memory addresses: (1) The physical address space allocated at initialization for UC communication or “**command page**”, and (2) The virtual address space used for data exchange or “**data page**”. The former is managed in the **FLR**, while the latter is included in the command field (Fig. 8) by the microservice application to initiate requests to be handled in the accelerators’ **RLR**.

Configuration Channel. *Arcalís* configuration mechanism establishes runtime communication with CPU cores. The OS specifies the physical address range the accelerator monitors for uncacheable (UC) memory requests. Any UC store or load within this range is intercepted and interpreted as an accelerator command. In practice, this configuration can be conveyed via PCIe-mapped registers or modern CPU-accelerator primitives such as Intel’s ENQCMD, MOVDIR64B [79], or Arm’s System Register Interfaces [5]. *Arcalís*’ **FLR** design incorporates a *Snooping Command Interface* (SCI) depicted in Fig. 7a that monitors memory transactions issued by CPU cores. Any UC store or load targeting the configured watch range is intercepted and interpreted as an accelerator command. When the kernel driver allocates a UC page for communication, it passes the virtual address to the application and the physical address to *Arcalís*, with which it programs the traffic snooping watch range. The SCI filters CPU memory operations that are (1) marked UC and (2) fall within the configured range. Moreover, *Arcalís*’ kernel driver pins the *command page*, preventing the OS

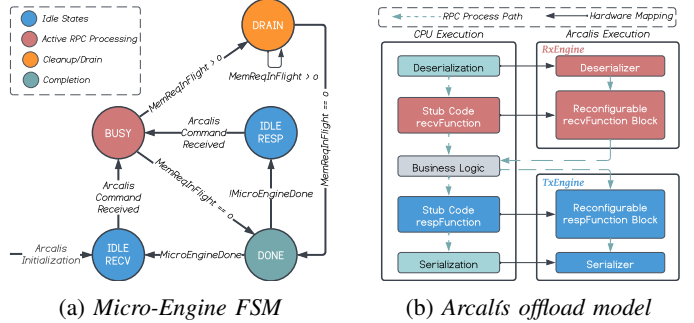


Fig. 9: *Arcalís* accelerator design: (a) state transitions, (b) *Arcalís* software to hardware mapping.

from changing it. As configuration occurs only once during initialization, its overhead is negligible.

Arcalís also exposes six lightweight control commands shown in Table III that facilitate communication between user-space microservices and the accelerator through the UC page. We found that these commands were sufficient to capture the communication requirements of representative microservices [28]. Each accelerator request is encoded within a 64-bit word, as illustrated in Figure 8: the upper 60 bits carry the data buffer address or length, while the lower 4 bits specify the *OpCode* corresponding to the command type.

Memory Management. *Arcalís* includes full virtual memory support to reduce access latency and enable direct interaction with data exchange buffers. Address translation operates in timing mode to model realistic MMU delays, including TLB misses and page table walks. The page table walker supports 4KB and 2MB data page. Virtual-to-Physical address translations are cached in a dedicated TLB (Figure 7a), which accelerates repeated accesses to hot buffers—critical for RPC workloads that exhibit strong temporal locality. Upon accessing an unmapped address, *Arcalís*’ translation unit reports a fault to the application. An error code is sent as a response to the pending UC load, so the application retries, triggering the CPU to touch the addresses and the OS to populate the page before *Arcalís* resumes.

b) **Reconfigurable Logic Region**: Hosts the programmable components of *Arcalís*. Operating in the *virtual address space*, it enables rapid adaptation to evolving RPC frameworks and microservice protocols as well as enables accelerators’ customization for efficiency. The RLR mainly consists of the RxEngine and TxEngine, as well as their control FSMs. The central FSM in Fig. 7a is a simple control block that identifies the command type (Table III, and consequently activates the micro-engines. Because application needs are dynamic, we position the Byte Selector (selects 4-bit command range) and the response Forward Unit in the RLR.

State Machine Architecture. Figure 9a depicts the RxEngine and TxEngine state machines, which orchestrate deterministic RPC execution across five states. The engine starts in IDLE_RECV state at initialization. Upon receiving a valid request, it transitions to BUSY, where it

performs core RPC operations such as header parsing/creation, serialization via the micro-engines. If outstanding memory operations remain, the engine moves to a separate DRAIN state to ensure all stores complete before finalizing via `MemReqInFlight`, to prevent data loss. Once execution completes, the engine enters DONE to trigger response back to the core and cleanup, followed by a transition to either IDLE_RESP (if the engines still have work to do) or back to IDLE_RECV to await the next RPC. This fine-grained state separation allows overlapping memory and compute phases, improving pipeline efficiency and RPC throughput.

Specializing IDL-driven De(Serialization). *Arcalís* offloads both the IDL-generated stub code and the core RPC data transformation logic to hardware. As shown in Figure 9b, the stub code (`recvFunction` and `respFunction`), as well as the De(serialization) operations are mapped into the RxEngine on the receive path and the TxEngine on the response path. These engines execute only the code produced by the IDL compiler, while specialized hardware units handle serialization and deserialization. To maintain a lightweight accelerator design, *Arcalís* derives these (de)serialization units directly from the IDL schema, implementing the data-movement and format-conversion logic in hardware. By placing these units in the **RLR**, *Arcalís* allows for flexibility while enabling efficient data transformation.

This hardware-software partitioning preserves RPC semantics while eliminating the instruction and control overhead inherent in software-based de(serialization).

```

1  /* NetCore thread */
2  while (true) {
3      receive_packet(&recv_buf);
4      netCallEngineWrite(net_recv_buf, recv_len);
5      netCallEngineRead(net_resp_buf);
6      send_packet(resp_buf);
7  }
8  /* AppCore thread */
9  for (bool done = false; !done;) {
10     appCallEngineRead(app_recv_buf);
11     ComposeUniqueId();
12     appCallEngineWrite(app_resp_buf, resp_len);
13 }

```

Listing 1: Per-core software integration with *Arcalís*.

Software Execution Model. Listing 1 demonstrates *Arcalís*' software execution model where network and application processing are distributed across separate CPU cores, following fundamental specialization principles established in high-performance networking systems [7], [61]. The NetCore thread manages packet I/O through DPDK-style interfaces (`receive_packet`, `send_packet`) [16] and coordinates with the accelerator via `netCallEngineWrite` and `netCallEngineRead` functions for data buffer exchange. Simultaneously, the AppCore thread focuses exclusively on business logic execution (`ComposeUniqueId`), accessing serialized RPC data through `appCallEngineRead` and writing responses via `appCallEngineWrite` primitives. The NetCore executes in a continuous loop similar to DPDK's `rte_eth_rx_burst()` [16], while the AppCore uses a bounded loop like in Thrift's `TConnectedClient::run()` [3].

While the example uses a NetCore with optimized

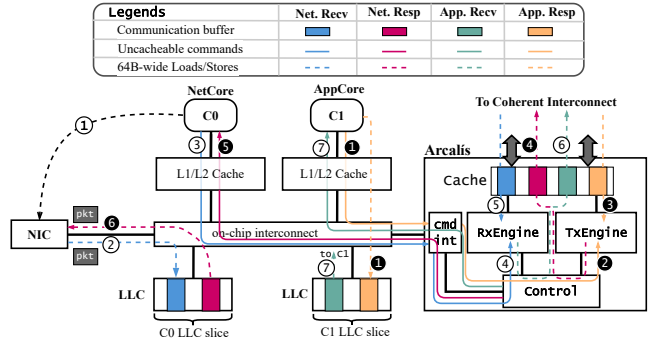


Fig. 10: End-To-End RPC Processing through *Arcalís*.

userspace networking for illustration, *Arcalís* can operate with hardware-terminated transport protocols [71] and hardware-accelerated NICs [25] that eliminate the need for dedicated network processing cores. In such configurations, the accelerator can directly interface with the network hardware, further reducing CPU overhead and enabling even tighter integration between network processing and RPC acceleration.

C. The End-to-End RPC Execution Pipeline

Figure 10 illustrates the detailed data and control flow involved in end-to-end RPC execution through *Arcalís*. The system comprises a Network Core (NetCore), an Application Core (AppCore), and the *Arcalís* accelerator, all connected via a coherent on-chip interconnect and sharing a unified LLC. Communication is mediated through four shared buffers—*Net. Recv*, *Net. Resp*, *App. Recv*, and *App. Resp*.

The architecture fully leverages the I/O data placement capabilities of modern CPUs that enable I/O devices to directly place their data into the CPU's caches [2], [6], [34]. Next, we discuss the life cycle of an RPC packet in *Arcalís*.

a) Receive Path Processing: The receive path begins at ① when the NetCore polls the NIC for incoming packets. Upon packet arrival (②), the data is DCA-ed from the NIC's on-chip SRAM buffer directly to any of NetCore's LLC DCA ways, corresponding to the *Net. Recv* buffer. This DCA-enabled transfer bypasses main memory, ensuring that packet data resides in the cache hierarchy for immediate processing. At ③, the NetCore issues a UC store to Arcalis, writing a command descriptor containing the address of the packet and relevant metadata. This command is received by the *Arcalís* control block (④), where it is decoded and passed to the central control FSM. The FSM activates the RxEngine, which begins executing the receive-side pipeline.

In ⑤, the RxEngine uses the address and length from the command to issue cache-coherent loads to retrieve the packet contents from the *Net. Recv* buffer. This action is facilitated by the TLB/MMU, and a load queue to issue accesses, while the ROB ensures a correct in-order retirement of memory transactions. The deserializer extracts the RPC function ID, and the dispatch module selects the appropriate `recvFunctionN` logic block.

At ⑥, the deserialized payload is written into the *App. Recv* buffer and control logic is updated to indicate readiness.

TABLE IV: *Simulation Baseline Configuration*

Component	Configuration
CPU Type	Out-of-Order, 8-wide issue/commit, 4 GHz
Instruction Fetch	64-entry fetch buffer, 8-wide fetch/decode
Branch Predictor	Tournament: 8K global/local, 2-bit counters
Caches	L1I/D: 32 KiB, 8-way, L2: 512 KiB, 8-way L3: 32 MiB (8 slices), 16-way
Memory	DDR4-2400, 3 GiB, 64-byte interleaving
Topology	2D Mesh, 1-cycle latency per hop
<i>Arcalís</i>	<i>Freq</i> : 1GHz ² , <i>Cache</i> : 512KiB, 8-way assoc

In ⑦, the *AppCore* performs an UC load when it is ready to process a request. *Arcalís* will respond with status metadata upon the successful writing of the payload, thereby completing the receive path. The application then begins business logic processing by issuing a load request to retrieve the contents of *App. Rcv* buffer ⑦.

b) Response Path Processing: Once the microservice function (business logic) completes execution, the *AppCore* writes its output into the *App. Resp* buffer. At ①, it signals *Arcalís* by issuing an uncacheable store containing the address and metadata of the response payload. The command reaches *Arcalís* in ②, where it is decoded and routed to the control logic, which activates the *TxEngine*.

In ③, the *TxEngine* accesses the application’s response buffer via cache-coherent loads, using the load queue, ROB, and virtual-to-physical address translation units (TLB/MMU) as in the receive path. Once data retrieval completes, the engine begins header creation and serialization tasks to transform the in-memory application data into wire format.

Following RPC processing in the *TxEngine*, it is written to the *Net. Resp* buffer in ④. At ⑤, the *NetCore* issues a UC load to query *Arcalís* for response readiness. *Arcalís* responds with a completion token, in the same manner it does to *AppCore* in the receive path. Finally, in coordination with the userspace networking library and hardware NIC driver, the response is DCA-ed from the *Net. Resp* buffer to the NIC’s on-chip SRAM ⑥, from where the packet response is transmitted over the network, completing the full RPC round-trip.

This end-to-end design enables *Arcalís* to efficiently process RPCs with zero-copy communication through the cache hierarchy, completely removing the CPU from the latency-sensitive control plane. *Arcalís* seamlessly integrates with existing RPC load balancing [15], [32], [66] and affinity-based steering mechanisms [63]. Unlike NIC-attached accelerators that require multiple memory traversals and CPU assistance, *Arcalís* accesses memory as efficiently as CPU cores while operating independently. This eliminates memory-affinity optimizations required by distant accelerators and frees cores entirely for application logic execution.

V. METHODOLOGY

We evaluate *Arcalís* by offloading RPC logic from key microservices to a near-cache accelerator. Our experiments use full-system gem5 [8], extending a reconfigurable accelerator framework [55] for integrating domain-specific hardware.

²The embedded FPGA demonstrated a maximum frequency of 1 GHz [21].

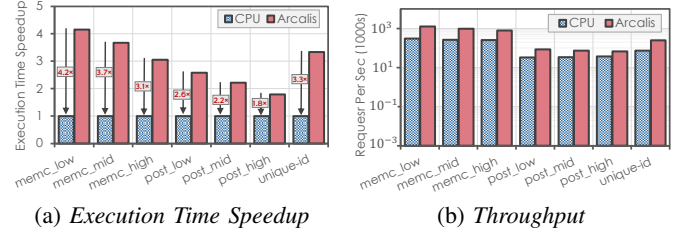


Fig. 11: End-to-end performance comparison showing normalized runtime for CPU baseline.

A. Simulation Setup

We use gem5 with Ubuntu 22.04. The system boots under KVM for fast initialization and then switches to a detailed out-of-order (O3) core for cycle-accurate execution. The accelerator is instantiated as a tile on a 2D mesh NoC and placed near the LLC to reduce communication latency. The baseline uses an 8-wide, 4 GHz O3 core with private L1/L2 caches and a multi-slice shared L3. Applications are pinned to dedicated cores. We compare *Arcalís* against a CPU-only baseline and prior RPC acceleration work. Full system parameters is shown in Table IV.

B. Microservice Workloads & Configuration

We evaluate three microservices built on the Thrift RPC framework: *Memcached* [51], *PostStorageService*, and *UniqueIdService*. Each application interfaces with *Arcalís* as described in §IV-B, offloading RPC parsing and dispatch logic to the accelerator. Following prior work [63], [73], we collect real-system traces and replay them in simulation to isolate RPC acceleration effects. Our setup emulates a network interface that DMAAs packet data into the CPU’s caches before triggering RPC processing via *Arcalís*.

Table V shows the evaluated workload configurations, characterized by write operation intensity (SET for *Memcached* and StorePost for *PostStorageService*):

TABLE V: *Microservice workloads configurations*.

Microservice	Operation Types	Workload Ratio (%)
<i>Memcached</i>	SET / GET (Zipfian Distribution)	<i>memc_low</i> : 20 / 80 <i>memc_mid</i> : 50 / 50 <i>memc_high</i> : 80 / 20 <i>memc_tiny</i> : k8_v8 <i>memc_small</i> : k16_v32
<i>PostStorageService</i>	StorePost / ReadPost / ReadPosts	<i>post_low</i> : 10 / 50 / 40 <i>post_mid</i> : 33 / 33 / 33 <i>post_high</i> : 90 / 5 / 5
<i>UniqueIdService</i>	ComposeUniqueId	<i>unique_id</i> : N/A

VI. EVALUATION

A. End-To-End RPC Acceleration

We first evaluate *Arcalís*’s overall performance impact by measuring end-to-end execution time and throughput across all microservice workloads. Figure 11a shows *Arcalís* achieves substantial end-to-end speedups across all workloads, ranging from 1.79 \times to 4.16 \times over the CPU baseline. *Memcached* workloads exhibit the highest acceleration, achieving 4.16 \times , 3.68 \times , and 3.05 \times for low, mid, and high write intensities, with speedups inversely correlated to write ratio. This trend reflects SET operations’ higher serialization overhead compared to GET operations. *PostStorageService* achieves

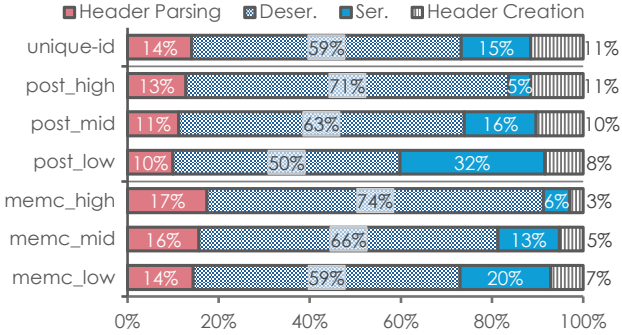


Fig. 12: Fraction of cycles spent in processing Core RPC operations. Dispatch stage is included to Deser. for simplicity.

2.58×, 2.21×, and 1.79× speedups respectively, with lower absolute gains due to its greater business logic complexity; a larger fraction of execution time resides in non-acceleratable application code [28]. *UniqueIdService* demonstrates a 3.33× speedup, confirming *Arcalís*’s effectiveness for lightweight, RPC-intensive services where protocol processing dominates total execution time.

Figure 11b presents the corresponding throughput improvements, measured in Thousand requests per second (trps). *Arcalís* delivers 74–247K rps compared to the CPU baseline’s 25–84K rps, yielding a throughput increase of 2.5–3.3×. The throughput scaling mirrors the speedup trends: *Memcached* achieves the highest throughput (248K, 202K, 258K req/s for low/mid/high), while *PostStorageService*’s heavier business logic yields lower but still significant gains (74–128K req/s). These results demonstrate that *Arcalís* effectively mitigates the RPC tax across diverse microservice characteristics, with acceleration benefits scaling proportionally to RPC processing intensity [70].

B. Arcalís Processing Time Breakdown

To understand how *Arcalís* distributes RPC work across its hardware pipeline, Figure 12 shows the processing time breakdown within the accelerator. RxEngine handles header parsing and deserialization, while TxEngine manages serialization and header creation. Deserialization dominates at 59%–74%, which translates to the RxEngine consuming 73%–91% of the total accelerator cycles. This trend is most pronounced in write-heavy workloads like *memc_high* and *post_high*, while read-intensive workloads like *memc_low* and *post_low* show more balanced engine profile. The high deserialization cost stems from heavy data movement requirements on the receive path, whereas serialization remains lower as response packets are typically smaller [45].

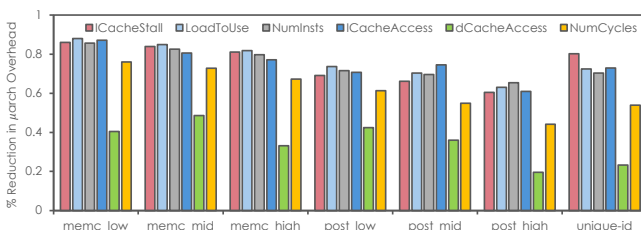


Fig. 13: CPU microarchitectural metrics showing reductions in instruction count, cache stalls, memory accesses, and execution cycles with *Arcalís*.

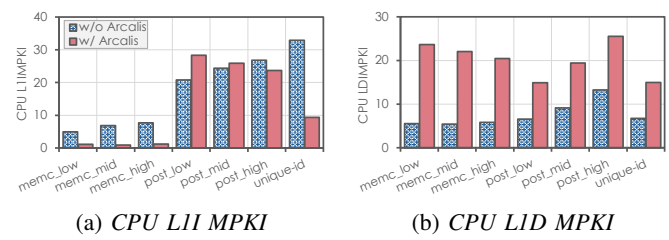


Fig. 14: CPU L1 instruction and data cache MPKI.

C. Microarchitectural Analysis

Figure 13 quantifies the effect of *Arcalís* on core microarchitectural behavior. Instruction count drops by 65.4% to 85.7% and cycle count by 44.2% to 76.0%, showing that offloaded RPC work directly reduces CPU execution time. Instruction cache accesses fall by 61.0% to 87.2%, while data cache accesses decrease by 19.6% to 48.6%. This reflects that *Arcalís* removes instruction-heavy parsing and marshaling, whereas data movement for application logic remains on the CPU. Read-intensive workloads such as *memc_low*, *memc_mid*, and *unique_id* see the largest data cache reductions at 42.4%, 48.8%, and 40.5%. LoadToUse latency improves by 63.1% to 88.0% and instruction cache stalls reduce by 60.5% to 86.1%, indicating fewer dependencies and a shorter critical path once RPC handling is offloaded. Overall, *Arcalís* substantially reduces front-end and back-end overheads and frees CPU resources for application work.

Figure 14 shows the corresponding L1 MPKI behavior. L1I MPKI decreases from 4.9 to 32.8 in the baseline (without *Arcalís*) to 0.9 to 28.3 with *Arcalís*, consistent with the large reduction in instruction-stream pressure. In contrast, L1D MPKI increases from 5.4 to 13.3 without *Arcalís* to 14.9 to 25.5 with *Arcalís*. This behavior is expected as *Arcalís* reduces total retired instructions by 3 to 6×, while the remaining code is more pointer- and data-intensive. Because MPKI is normalized by instruction count, the smaller dynamic footprint causes the residual data misses to form a larger fraction of normalized activity. The higher L1D MPKI therefore reflects a shifted instruction mix rather than a performance degradation.

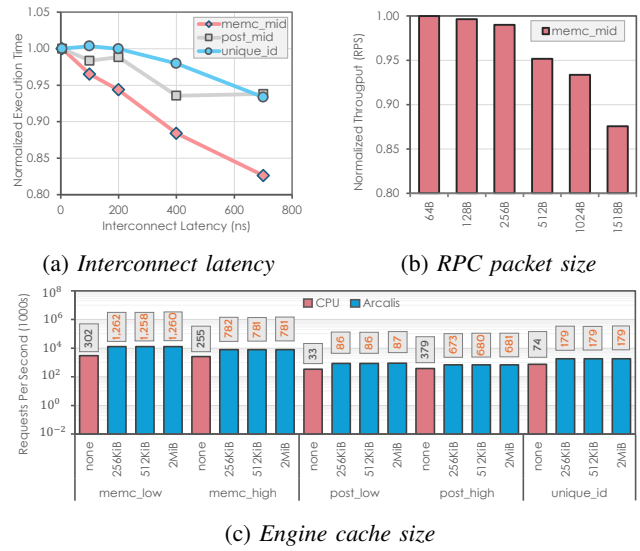


Fig. 15: Sensitivity analysis under varying (a) RPC packet sizes, (b) interconnect latencies, and (c) engine cache sizes.

D. Sensitivity Analysis

Figure 15a reports the sensitivity of *Arcalis* to CPU–accelerator interconnect latency. Increasing the communication delay from 5 ns to 400 ns raises execution time by 8–13% for *Memcached* and less than 7% for *PostStorageService* and *UniqueIdService*. At 700 ns, which approximates a PCIe traversal, the slowdown reaches 21% for *Memcached* and stays below 10% for the other workloads. Figure 15b shows the corresponding sensitivity to RPC packet size: *Memcached* throughput decreases by 7% at 512 B, 12% at 1024 B, and 16% at 1518 B. These overheads remain well within the overall 1.8–4.2× performance gains provided by *Arcalis*, indicating that neither interconnect latency nor packet size materially affects the benefits of near-cache RPC offload.

We also sweep the accelerator’s local cache capacity to assess sensitivity to RPC working-set size. As shown in Figure 15c, throughput rises substantially once a small cache is available, with 256 KiB already capturing the working sets for all workloads. Increasing the cache to 512 KiB or 2 MiB produces no measurable improvement, indicating that the hot RPC state accessed by the engines is well under a few hundred kilobytes. These results show that *Arcalis* requires only a modest private cache to sustain its performance.

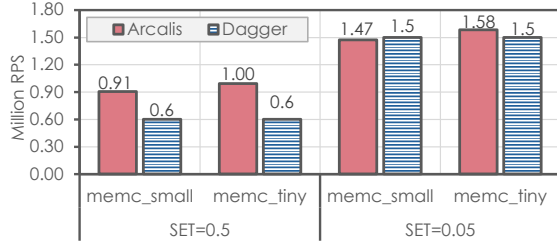


Fig. 16: Throughput comparison between *Arcalis* and Dagger. E. Comparison to Prior Works

Figure 16 compares *Arcalis* with Dagger [45] under *Memcached* workloads using the same key–value sizes and SET/GET mixes reported in prior work. For SET=0.5, *Arcalis* sustains 0.91 MRPS on *memc_small* and 1.00 MRPS on *memc_tiny*, corresponding to 1.52× and 1.67× higher throughput than Dagger’s 0.6 MRPS on both workloads. At the lighter SET=0.05 mix, the two systems perform similarly: *Arcalis* reaches 1.47 MRPS and 1.58 MRPS, while Dagger reports 1.5 MRPS, yielding 0.98× and 1.05× throughput relative to Dagger. These results show that *Arcalis* provides substantial gains for write-intensive RPCs and matches state-of-the-art performance in read-heavy configurations.

RpcNIC [80] offers another point of comparison. It reports a 1.4× speedup on the *unique_id* service from DeathStarBench [28], while *Arcalis* reaches 3.33× on the same workload. The higher gain comes from performing RPC parsing and dispatch in the near-cache region and avoiding PCIe traversal, which lowers offload overheads without specialized memcpy engines [14], [44].

F. Power and Area Analysis

Our prototype of the *Memcached* accelerator on an AMD xa7a12tcp238-2i FPGA uses 5,706 LUTs, 5,609 FFs, and

32 CARRY8 units. These resources are equivalent to 2.83 mm² because a 4.34 mm² silicon area can accommodate 2,190 compute elements (CEs), each containing 4 LUTs, 8 FFs, and 1 CARRY8 [46]. The total power is 379 mW, including 263 mW of dynamic power. The area of a typical 8-core system is 23.52 mm² [46]. Therefore, the total area of a system with *Arcalis* is 26.35 mm². Although other services require different FSMs, their overheads remain similar since FSMs occupy a small portion of the accelerator. Other components, implemented as ASICs, are negligible compared to a core.

VII. RELATED WORK

RPC and Microservice Acceleration. Prior RPC acceleration efforts span software optimizations and specialized hardware. Software approaches include kernel-bypass frameworks like eRPC [38], FaSST [39], and DPDK-based solutions [7], [50], [64], which reduce OS overhead but remain CPU-intensive. Hardware accelerators take diverse approaches: NIC-attached designs (Cerebros [63], Optimus Prime [62], NeBuLa [71]) offload RPC processing to smart NICs but suffer from fixed-function limitations and network traversal latency. FPGA-based solutions like Dagger [45] and RpcNIC [80] offer flexibility but face interconnect bottlenecks (400ns UPI, 900ns PCIe respectively). *Arcalis* uniquely combines near-cache placement with programmability, avoiding both interconnect penalties and deployment barriers while delivering superior microarchitectural improvements.

Near-Memory and Cache-Adjacent Computing. Near-memory computing has gained traction for data-intensive workloads [43], [68]. Processing-in-memory (PIM) designs like Samsung’s HBM-PIM [47] and UPMEM [53] place compute units within memory modules, while near-data accelerators [18], [56], [76] and [35] position specialized logic adjacent to the cache. Cache-conscious designs include directory caches [74], near-cache prefetchers [17], [31], and coherence accelerators [9]. However, these approaches target compute-intensive kernels or memory bandwidth optimization rather than protocol processing. *Arcalis* extends this paradigm by demonstrating that near-cache placement effectively addresses RPC’s memory access latency and cache inefficiencies.

VIII. CONCLUSIONS

This paper presented *Arcalis*, the first near-cache RPC accelerator that addresses fundamental microservice performance bottlenecks by positioning lightweight hardware engines adjacent to the last-level cache. *Arcalis* achieves 1.79–4.16× end-to-end speedups while significantly reducing front-end and backend inefficiencies. Unlike existing approaches that require specialized hardware or sacrifice flexibility, *Arcalis* integrates with commodity processors while maintaining programmability for evolving microservice environments. As microservices continue to dominate datacenter architectures, near-cache RPC offload provides a practical and deployable path to overcoming the RPC tax and unlocking higher CPU efficiency.

REFERENCES

[1] M. Alian and N. S. Kim, "Netdimm: Low-latency near-memory network interface architecture," in *Proceedings of the 52nd Annual IEEE/ACM International Symposium on Microarchitecture*, 2019, pp. 699–711.

[2] AMD, "Smart Data Cache Injection (SDCI) white paper" <https://www.amd.com/content/dam/en/documents/epyc-technical-docs/white-papers/58725.pdf>, accessed: 2025-7-25.

[3] Apache Software Foundation, "TConnectedClient.cpp," 2025, line 55, Accessed: 2025-07-26. [Online]. Available: <https://github.com/apache/thrift/blob/master/lib/cpp/src/thrift/server/TConnectedClient.cpp#L55>

[4] Apache Thrift Software Framework, "thrift.org," 2025, accessed: 2025-07-26. [Online]. Available: <https://thrift.apache.org/>

[5] Arm, "CP14 and CP15 system control registers," 2025, arm Developer Documentation, Accessed: 2025-07-26. [Online]. Available: <https://developer.arm.com/documentation/ddi0406/cb/System-Level-Architecture/The-System-Level-Programmers-Model/Coprocessors-and-system-control/CP14-and-CP15-system-control-registers?lang=en>

[6] Arm Limited, "Cache stashing," 2025, arm Developer Documentation, Accessed: 2025-07-26. [Online]. Available: <https://developer.arm.com/documentation/102407/0102/Cache-stashing>

[7] A. Belay, G. Prekas, A. Klimovic, S. Grossman, C. Kozyrakis, and E. Bugnion, "{IX}: a protected dataplane operating system for high throughput and low latency," in *11th USENIX Symposium on Operating Systems Design and Implementation (OSDI 14)*, 2014, pp. 49–65.

[8] N. Binkert, B. Beckmann, G. Black, S. K. Reinhardt, A. Saidi, A. Basu, J. Hestness, D. R. Hower, T. Krishna, S. Sardashti, R. Sen, K. Sewell, M. Shoaib, N. Vaish, M. D. Hill, and D. A. Wood, "The gem5 simulator," *SIGARCH Comput. Archit. News*, vol. 39, no. 2, p. 1–7, Aug. 2011. [Online]. Available: <https://doi.org/10.1145/2024716.2024718>

[9] A. Boroumand, S. Ghose, M. Patel, H. Hassan, B. Lucia, R. Ausavarungnirun, K. Hsieh, N. Hajinazar, K. T. Malladi, H. Zheng *et al.*, "Conda: Efficient cache coherence support for near-data accelerators," in *Proceedings of the 46th International Symposium on Computer Architecture*, 2019, pp. 629–642.

[10] Q. Cai, S. Chaudhary, M. Vuppala, J. Hwang, and R. Agarwal, "Understanding host network stack overheads," in *Proceedings of the 2021 ACM SIGCOMM 2021 Conference*, ser. SIGCOMM '21. New York, NY, USA: Association for Computing Machinery, 2021, p. 65–77. [Online]. Available: <https://doi.org/10.1145/3452296.3472888>

[11] Cap'n Proto, "Cap'n Proto - Infinitely Fast Serialization," 2025, accessed: 2025-07-26. [Online]. Available: <https://capnproto.org/>

[12] A. M. Caulfield, E. S. Chung, A. Putnam, H. Angepat, J. Fowers, M. Haselman, S. Heil, M. Humphrey, P. Kaur, J.-Y. Kim *et al.*, "A cloud-scale acceleration architecture," in *2016 49th Annual IEEE/ACM international symposium on microarchitecture (MICRO)*. IEEE, 2016, pp. 1–13.

[13] S. Chen, S. GalOn, C. Delimitrou, S. Manne, and J. F. Martínez, "Workload characterization of interactive cloud services on big and small server platforms," in *2017 IEEE International Symposium on Workload Characterization (IISWC)*, 2017, pp. 125–134.

[14] I. Corporation, "Intel Data Streaming Accelerator," 2025, accessed: 2025-07-26. [Online]. Available: <https://www.intel.com/content/www/us/en/products/docs/accelerator-engines/data-streaming-accelerator.html>

[15] A. Daglis, M. Sutherland, and B. Falsafi, "Rpvale: Ni-driven tail-aware balancing of us-scale rpcs," in *Proceedings of the Twenty-Fourth International Conference on Architectural Support for Programming Languages and Operating Systems*, ser. ASPLOS '19. New York, NY, USA: Association for Computing Machinery, 2019, p. 35–48. [Online]. Available: <https://doi.org/10.1145/3297858.3304070>

[16] Data Plane Development Kit, "DPDK.org," 2025, accessed: 2025-07-26. [Online]. Available: <https://www.dpdk.org/>

[17] D. Deb, J. Jose, and M. Palesi, "Performance enhancement of caches in tcmps using near vicinity prefetcher," in *2019 32nd International Conference on VLSI Design and 2019 18th International Conference on Embedded Systems (VLSID)*. IEEE Computer Society, 2019, pp. 13–18.

[18] A. Denzler, G. F. Oliveira, N. Hajinazar, R. Bera, G. Singh, J. Gómez-Luna, and O. Mutlu, "Casper: Accelerating stencil computations using near-cache processing," *IEEE Access*, vol. 11, pp. 22 136–22 154, 2023.

[19] A. Dragojević, D. Narayanan, M. Castro, and O. Hodson, "{FaRM}: Fast remote memory," in *11th USENIX Symposium on Networked Systems Design and Implementation (NSDI 14)*, 2014, pp. 401–414.

[20] D. Duplyakin, R. Ricci, A. Maricq, G. Wong, J. Duerig, E. Eide, L. Stoller, M. Hibler, D. Johnson, K. Webb, A. Akella, K. Wang, G. Ricart, L. Landweber, C. Elliott, M. Zink, E. Cecchet, S. Kar, and P. Mishra, "The design and operation of CloudLab," in *Proceedings of the USENIX Annual Technical Conference (ATC)*, Jul. 2019, pp. 1–14. [Online]. Available: <https://www.flux.utah.edu/paper/duplyakin-atc19>

[21] EDN, "Flex logix high-performance embedded fpga ip core," <https://www.edn.com/flex-logix-high-performance-embedded-fpga-ip-core-now-available-for-tsmc-16ff-and-16ffc/>, accessed: 2025-11-15.

[22] H. Eran, L. Zeno, M. Tork, G. Malka, and M. Silberstein, "{NICA}: An infrastructure for inline acceleration of network applications," in *2019 USENIX Annual Technical Conference (USENIX ATC 19)*, 2019, pp. 345–362.

[23] H. Esmaeilzadeh, E. Blem, R. St. Amant, K. Sankaralingam, and D. Burger, "Dark silicon and the end of multicore scaling," in *Proceedings of the 38th annual international symposium on Computer architecture*, 2011, pp. 365–376.

[24] A. Farshin, A. Roozbeh, G. Q. Maguire Jr, and D. Kostić, "Reexamining direct cache access to optimize {I/O} intensive applications for multi-hundred-gigabit networks," in *2020 USENIX Annual Technical Conference (USENIX ATC 20)*, 2020, pp. 673–689.

[25] D. Firestone, A. Putnam, S. Mundkur, D. Chiou, A. Dabagh, M. Andrewartha, H. Angepat, V. Bhanu, A. Caulfield, E. Chung *et al.*, "Azure accelerated networking:{SmartNICs} in the public cloud," in *15th USENIX Symposium on Networked Systems Design and Implementation (NSDI 18)*, 2018, pp. 51–66.

[26] J. Fried, Z. Ruan, A. Oosterhout, and A. Belay, "Caladan: Mitigating interference at microsecond timescales," in *14th USENIX Symposium on Operating Systems Design and Implementation (OSDI 20)*, 2020, pp. 281–297.

[27] Y. Gan and C. Delimitrou, "The architectural implications of cloud microservices," *IEEE Computer Architecture Letters*, vol. 17, no. 2, pp. 155–158, 2018.

[28] Y. Gan, Y. Zhang, D. Cheng, A. Shetty, P. Rathi, N. Katarki, A. Bruno, J. Hu, B. Ritchken, B. Jackson, K. Hu, M. Pancholi, Y. He, B. Clancy, C. Colen, F. Wen, C. Leung, S. Wang, L. Zaruvinsky, M. Espinosa, R. Lin, Z. Liu, J. Padilla, and C. Delimitrou, "An open-source benchmark suite for microservices and their hardware-software implications for cloud & edge systems," ser. ASPLOS '19. New York, NY, USA: Association for Computing Machinery, 2019, p. 3–18. [Online]. Available: <https://doi.org/10.1145/3297858.3304013>

[29] S. Ghose, A. Boroumand, J. S. Kim, J. Gómez-Luna, and O. Mutlu, "Processing-in-memory: A workload-driven perspective," *IBM Journal of Research and Development*, vol. 63, no. 6, pp. 3–1, 2019.

[30] gRPC, "gRPC - A high performance, open source universal RPC framework," 2025, accessed: 2025-07-26. [Online]. Available: <https://grpc.io/>

[31] W. Heirman, K. D. Bois, Y. Vandriessche, S. Eyerman, and I. Hur, "Near-side prefetch throttling: Adaptive prefetching for high-performance many-core processors," in *Proceedings of the 27th international conference on parallel architectures and compilation techniques*, 2018, pp. 1–11.

[32] J. Huang, J. Lou, S. Vanavasam, X. Kong, H. Ji, I. Jeong, D. Zhuo, E. K. Lee, and N. S. Kim, "Hal: Hardware-assisted load balancing for energy-efficient snic-host cooperative computing," in *2024 ACM/IEEE 51st Annual International Symposium on Computer Architecture (ISCA)*. IEEE, 2024, pp. 613–627.

[33] D. Huye, Y. Shkuro, and R. R. Sambasivan, "Lifting the veil on {Meta's} microservice architecture: Analyses of topology and request workflows," in *2023 USENIX Annual Technical Conference (USENIX ATC 23)*, 2023, pp. 419–432.

[34] Intel Corporation, "Intel Data Direct I/O Technology," Intel Corporation, Technology Brief, 2025, accessed: 2025-07-26. [Online]. Available: <https://www.intel.com/content/dam/www/public/us/en/documents/technology-briefs/data-direct-i-o-technology-brief.pdf>

[35] Ş. İzmirli, J. Pavon, I. V. Valdivieso, B. Aydeğer, K. Yalçınkaya, A. Cristal, O. Ergin, and O. Ünsal, "Halis: A hardware-software co-designed near-cache accelerator for graph pattern mining," *IEEE Computer Architecture Letters*, 2025.

[36] E. Jeong, S. Wood, M. Jamshed, H. Jeong, S. Ihm, D. Han, and K. Park, "{mTCP}: a highly scalable user-level {TCP} stack for multicore systems," in *11th USENIX Symposium on Networked Systems Design and Implementation (NSDI 14)*, 2014, pp. 489–502.

[37] A. Joosen, A. Hassan, M. Asenov, R. Singh, L. Darlow, J. Wang, Q. Deng, and A. Barker, “Serverless cold starts and where to find them,” ser. EuroSys ’25. New York, NY, USA: Association for Computing Machinery, 2025, p. 938–953. [Online]. Available: <https://doi.org/10.1145/3689031.3696073>

[38] A. Kalia, M. Kaminsky, and D. Andersen, “Datacenter {RPCs} can be general and fast,” in *16th USENIX Symposium on Networked Systems Design and Implementation (NSDI 19)*, 2019, pp. 1–16.

[39] A. Kalia, M. Kaminsky, and D. G. Andersen, “FaSST: Fast, scalable and simple distributed transactions with two-sided (rdma) datagram RPCs,” in *12th USENIX Symposium on Operating Systems Design and Implementation (OSDI 16)*. Savannah, GA: USENIX Association, Nov. 2016, pp. 185–201. [Online]. Available: <https://www.usenix.org/conference/osdi16/technical-sessions/presentation/kalia>

[40] S. Kaney, J. P. Darago, K. Hazelwood, P. Ranganathan, T. Moseley, G.-Y. Wei, and D. Brooks, “Profiling a warehouse-scale computer,” in *Proceedings of the 42nd Annual International Symposium on Computer Architecture*, ser. ISCA ’15. New York, NY, USA: Association for Computing Machinery, 2015, p. 158–169. [Online]. Available: <https://doi.org/10.1145/2749469.2750392>

[41] S. Karandikar, C. Leary, C. Kennelly, J. Zhao, D. Parimi, B. Nikolic, K. Asanovic, and P. Ranganathan, “A hardware accelerator for protocol buffers,” in *MICRO-54: 54th Annual IEEE/ACM International Symposium on Microarchitecture*, 2021, pp. 462–478.

[42] M. Khairy, A. Alawneh, A. Barnes, and T. G. Rogers, “Simr: Single instruction multiple request processing for energy-efficient data center microservices,” in *2022 55th IEEE/ACM International Symposium on Microarchitecture (MICRO)*. IEEE, 2022, pp. 441–463.

[43] G. Kim, N. Chatterjee, M. O’Connor, and K. Hsieh, “Toward standardized near-data processing with unrestricted data placement for gpus,” in *Proceedings of the International Conference for High Performance Computing, Networking, Storage and Analysis*, 2017, pp. 1–12.

[44] R. Kuper, I. Jeong, Y. Yuan, R. Wang, N. Ranganathan, N. Rao, J. Hu, S. Kumar, P. Lantz, and N. S. Kim, “A quantitative analysis and guidelines of data streaming accelerator in modern intel xeon scalable processors,” in *Proceedings of the 29th ACM International Conference on Architectural Support for Programming Languages and Operating Systems, Volume 2*, 2024, pp. 37–54.

[45] N. Lazarev, S. Xiang, N. Adit, Z. Zhang, and C. Delimitrou, “Dagger: efficient and fast rpcs in cloud microservices with near-memory reconfigurable nics,” in *Proceedings of the 26th ACM International Conference on Architectural Support for Programming Languages and Operating Systems*, ser. ASPLOS ’21. New York, NY, USA: Association for Computing Machinery, 2021, p. 36–51. [Online]. Available: <https://doi.org/10.1145/3445814.3446696>

[46] S. K. Lee, P. N. Whatmough, M. Donato, G. G. Ko, D. Brooks, and G.-Y. Wei, “Smiv: A 16-nm 25-mm² soc for iot with arm cortex-a53, efgpa, and coherent accelerators,” *IEEE Journal of Solid-State Circuits*, vol. 57, no. 2, pp. 639–650, 2022.

[47] S. Lee, S.-h. Kang, J. Lee, H. Kim, E. Lee, S. Seo, H. Yoon, S. Lee, K. Lim, H. Shin *et al.*, “Hardware architecture and software stack for pim based on commercial dram technology: Industrial product,” in *2021 ACM/IEEE 48th Annual International Symposium on Computer Architecture (ISCA)*. IEEE, 2021, pp. 43–56.

[48] S. Li, H. Lim, V. W. Lee, J. H. Ahn, A. Kalia, M. Kaminsky, D. G. Andersen, O. Seongil, S. Lee, and P. Dubey, “Architecting to achieve a billion requests per second throughput on a single key-value store server platform,” in *Proceedings of the 42nd Annual International Symposium on Computer Architecture*, 2015, pp. 476–488.

[49] S. Luo, H. Xu, C. Lu, K. Ye, G. Xu, L. Zhang, Y. Ding, J. He, and C. Xu, “Characterizing microservice dependency and performance: Alibaba trace analysis,” in *Proceedings of the ACM Symposium on Cloud Computing*, ser. SoCC ’21. New York, NY, USA: Association for Computing Machinery, 2021, p. 412–426. [Online]. Available: <https://doi.org/10.1145/3472883.3487003>

[50] M. Marty, M. de Kruijf, J. Adriaens, C. Alfeld, S. Bauer, C. Contavalli, M. Dalton, N. Dukkipati, W. C. Evans, S. Gribble *et al.*, “Snap: A microkernel approach to host networking,” in *Proceedings of the 27th ACM Symposium on Operating Systems Principles*, 2019, pp. 399–413.

[51] Memcached, “Memcached - a distributed memory object caching system,” 2025, accessed: 2025-07-26. [Online]. Available: <https://github.com/memcached/memcached>

[52] A. Mirhosseini, A. Sriraman, and T. F. Wenisch, “Enhancing server efficiency in the face of killer microseconds,” in *2019 IEEE International Symposium on High Performance Computer Architecture (HPCA)*. IEEE, 2019, pp. 185–198.

[53] O. Mutlu, S. Ghose, J. Gómez-Luna, and R. Ausavarungnirun, “A modern primer on processing in memory,” in *Emerging computing: from devices to systems: looking beyond Moore and Von Neumann*. Springer, 2022, pp. 171–243.

[54] R. Neugebauer, G. Antichi, J. F. Zazo, Y. Audzevich, S. López-Buedo, and A. W. Moore, “Understanding pcie performance for end host networking,” in *Proceedings of the 2018 Conference of the ACM Special Interest Group on Data Communication*, ser. SIGCOMM ’18. New York, NY, USA: Association for Computing Machinery, 2018, p. 327–341. [Online]. Available: <https://doi.org/10.1145/3230543.3230560>

[55] H. Nguyen, P. Maidee, J. Lowe-Power, and A. Kaviani, “Choreographer: A full-system framework for fine-grained tasks in cache hierarchies,” 2025. [Online]. Available: <https://arxiv.org/abs/2510.26944>

[56] A. V. Nori, R. Bera, S. Balachandran, J. Rakshit, O. J. Omer, A. Abuhatzera, B. Kuttanna, and S. Subramoney, “Reducit: Keep it close, keep it cool!: Efficient scaling of dnn inference on multi-core cpus with near-cache compute,” in *2021 ACM/IEEE 48th Annual International Symposium on Computer Architecture (ISCA)*. IEEE, 2021, pp. 167–180.

[57] NVIDIA, “Benefits of RDMA over Routed Fabrics,” NVIDIA Corporation, Solution Brief, 2025, accessed: 2025-07-26. [Online]. Available: <https://network.nvidia.com/pdf/solutions/benefits-of-RDMA-over-routed-fabrics.pdf>

[58] NVIDIA, “Infiniband technology overview,” NVIDIA Corporation, White Paper, 2025, accessed: 2025-07-26. [Online]. Available: https://network.nvidia.com/pdf/whitepapers/WP_InfiniBand_Technology_Overview.pdf

[59] ———, “Rdma over converged ethernet (roce),” 2025, nVIDIA Networking Documentation, Accessed: 2025-07-26. [Online]. Available: [https://docs.nvidia.com/networking/display/mlnxofedv23070512/rdma+over+converged+ethernet+\(roce\)](https://docs.nvidia.com/networking/display/mlnxofedv23070512/rdma+over+converged+ethernet+(roce))

[60] A. Ousterhout, J. Fried, J. Behrens, A. Belay, and H. Balakrishnan, “Shenango: Achieving high {CPU} efficiency for latency-sensitive datacenter workloads,” in *16th USENIX Symposium on Networked Systems Design and Implementation (NSDI 19)*, 2019, pp. 361–378.

[61] S. Peter, J. Li, I. Zhang, D. R. Ports, D. Woos, A. Krishnamurthy, T. Anderson, and T. Roscoe, “Arrakis: The operating system is the control plane,” *ACM Transactions on Computer Systems (TOCS)*, vol. 33, no. 4, pp. 1–30, 2015.

[62] A. Pourhabibi, S. Gupta, H. Kassir, M. Sutherland, Z. Tian, M. P. Drumond, B. Falsafi, and C. Koch, “Optimus prime: Accelerating data transformation in servers,” in *Proceedings of the Twenty-Fifth International Conference on Architectural Support for Programming Languages and Operating Systems*, 2020, pp. 1203–1216.

[63] A. Pourhabibi, M. Sutherland, A. Daglis, and B. Falsafi, “Cerebros: Evading the rpc tax in datacenters,” in *MICRO-54: 54th Annual IEEE/ACM International Symposium on Microarchitecture*, ser. MICRO ’21. New York, NY, USA: Association for Computing Machinery, 2021, p. 407–420. [Online]. Available: <https://doi.org/10.1145/3466752.3480055>

[64] G. Prekas, M. Kogias, and E. Bugnion, “Zygos: Achieving low tail latency for microsecond-scale networked tasks,” in *Proceedings of the 26th Symposium on Operating Systems Principles*, 2017, pp. 325–341.

[65] K. Seemakupt, B. E. Stephens, S. Khan, S. Liu, H. Wassel, S. H. Yeganeh, A. C. Snoeren, A. Krishnamurthy, D. E. Culler, and H. M. Levy, “A cloud-scale characterization of remote procedure calls,” in *Proceedings of the 29th Symposium on Operating Systems Principles*, ser. SOSP ’23. New York, NY, USA: Association for Computing Machinery, 2023, p. 498–514. [Online]. Available: <https://doi.org/10.1145/3600006.3613156>

[66] H. Seyedroudbari, S. Vanavasam, and A. Daglis, “Turbo: Smartnic-enabled dynamic load balancing of μ s-scale rpcs,” in *2023 IEEE International Symposium on High-Performance Computer Architecture (HPCA)*. IEEE, 2023, pp. 1045–1058.

[67] Y. S. Shao, S. L. Xi, V. Srinivasan, G.-Y. Wei, and D. Brooks, “Co-designing accelerators and soc interfaces using gem5-aladdin,” in *2016 49th Annual IEEE/ACM International Symposium on Microarchitecture (MICRO)*, 2016, pp. 1–12.

[68] G. Singh, L. Chelini, S. Corda, A. J. Awan, S. Stuijk, R. Jordans, H. Corporaal, and A.-J. Boonstra, “A review of near-memory computing

architectures: Opportunities and challenges,” in *2018 21st Euromicro Conference on Digital System Design (DSD)*. IEEE, 2018, pp. 608–617.

[69] A. Skiadopoulos, Z. Xie, M. Zhao, Q. Cai, S. Agarwal, J. Adelmann, D. Ahern, C. Contavalli, M. Goldfam, V. Mayatskikh, R. Raja, D. Walton, R. Agarwal, S. Mukherjee, and C. Kozyrakis, “High-throughput and flexible host networking for accelerated computing,” in *18th USENIX Symposium on Operating Systems Design and Implementation (OSDI 24)*. Santa Clara, CA: USENIX Association, Jul. 2024, pp. 405–423. [Online]. Available: <https://www.usenix.org/conference/osdi24/presentation/skiadopoulos>

[70] A. Sriram and T. F. Wenisch, “ μ suite: a benchmark suite for microservices,” in *2018 ieee international symposium on workload characterization (iiswc)*. IEEE, 2018, pp. 1–12.

[71] M. Sutherland, S. Gupta, B. Falsafi, V. Marathe, D. Pnevmatikatos, and A. Daglis, “The nebula rpc-optimized architecture,” in *2020 ACM/IEEE 47th Annual International Symposium on Computer Architecture (ISCA)*, 2020, pp. 199–212.

[72] T. Ueda, T. Nakaike, and M. Ohara, “Workload characterization for microservices,” in *2016 IEEE International Symposium on Workload Characterization (IISWC)*, 2016, pp. 1–10.

[73] J. Umeike, S. Agarwal, N. Lazarev, and M. Alian, “Userspace networking in gem5,” in *2024 IEEE International Symposium on Performance Analysis of Systems and Software (ISPASS)*. IEEE, 2024, pp. 179–191.

[74] J. J. Valls, A. Ros, J. Sahuquillo, and M. E. Gómez, “Ps directory: A scalable multilevel directory cache for cmps,” *The Journal of Supercomputing*, vol. 71, no. 8, pp. 2847–2876, 2015.

[75] M. Wang, M. Xu, and J. Wu, “Understanding i/o direct cache access performance for end host networking,” *Proc. ACM Meas. Anal. Comput. Syst.*, vol. 6, no. 1, Feb. 2022. [Online]. Available: <https://doi.org/10.1145/3508042>

[76] Z. Wang, J. Weng, S. Liu, and T. Nowatzki, “Near-stream computing: General and transparent near-cache acceleration,” in *2022 IEEE International Symposium on High-Performance Computer Architecture (HPCA)*. IEEE, 2022, pp. 331–345.

[77] Wikipedia, “Common Object Request Broker Architecture,” 2025, accessed: 2025-07-26. [Online]. Available: https://en.wikipedia.org/wiki/Common_Object_Request_Broker_Architecture

[78] —, “Sun RPC,” 2025, accessed: 2025-07-26. [Online]. Available: https://en.wikipedia.org/wiki/Sun_RPC

[79] Y. Yuan, R. Wang, N. Ranganathan, N. Rao, S. Kumar, P. Lantz, V. Sanjeepan, J. Cabrera, A. Kwatra, R. Sankaran *et al.*, “Intel accelerators ecosystem: An soc-oriented perspective: Industry product,” in *2024 ACM/IEEE 51st Annual International Symposium on Computer Architecture (ISCA)*. IEEE, 2024, pp. 848–862.

[80] J. Zhang, H. Huang, X. Chen, X. Li, J. Zhao, M. Liu, and Z. Wang, “Rpcnic: Enabling efficient datacenter rpc offloading on pcie-attached smartnics,” in *2025 IEEE International Symposium on High Performance Computer Architecture (HPCA)*, 2025, pp. 1379–1394.

[81] Y. Zhang, Y. Gan, and C. Delimitrou, “jqsim: Enabling accurate and scalable simulation for interactive microservices,” in *2019 IEEE International Symposium on Performance Analysis of Systems and Software (ISPASS)*. IEEE, 2019, pp. 212–222.

[82] J. Zhao, I. Uwizeyimana, K. Ganesan, M. C. Jeffrey, and N. E. Jerger, “Altocumulus: Scalable scheduling for nanosecond-scale remote procedure calls,” in *2022 55th IEEE/ACM International Symposium on Microarchitecture (MICRO)*. IEEE, 2022, pp. 423–440.

[83] X. Zhou, X. Peng, T. Xie, J. Sun, C. Xu, C. Ji, and W. Zhao, “Benchmarking microservice systems for software engineering research,” in *Proceedings of the 40th International Conference on Software Engineering: Companion Proceedings*, 2018, pp. 323–324.